Electronic Supplementary Material (ESI) for Nanoscale.

Bio-engineered Nano-vesicles for IR820 Delivery: A Therapy Platform for Cancer by Surgery and Photothermal Therapy

Xiaojie Zhang,[#a,e] Changsheng Zhou,[#a,b,e] Fanghua Wu,[#d] Chang Gao,[a,e] Qianqian Liu,[a,e] Peng Lv,[a,e] Ming Li,[a,e] Liyong Huang,[*d] Ting Wu,[*a,c,e] Wengang Li,[*a,c,e]

[a] Department of Hepatobiliary Surgery, Xiang'an Hospital of Xiamen University, School of Medicine, Xiamen University, Xiamen, Fujian 361102, P. R. China. E-mail：lwgang@xmu.edu.cn
[b] Department of Hepatobiliary Surgery, Guizhou Provincial People's Hospital, Guiyang, Guizhou 550002, P. R. China.
c Cancer Research Center, School of Medicine, Xiamen University, Xiamen, Fujian 361102, P. R. China. E-mail：wuting78@189.cn
d Surgery department, Affiliated Fuzhou First Hospital of Fujian Medical University, Fuzhou, Fujian 350009, P. R. China. E-mail：40178404@qq.com
e Xiamen University Research Center of Retroperitoneal Tumor Committee of Oncology Society of Chinese Medical Association, Xiamen University, Xiamen, Fujian 361102, P. R. China.

# These authors contributed equally to this work.
* Corresponding authors

2. Results and discussion

Table S1. Recombinant plasmid sequence

Name	DNA sequence
Gas6	ATGGCCCCTTCGCTCTCGCCCGGGCCCGCCGCCCTGCGC CGCGCGCCGCAGCTGCTGCTGCTGCTGCTGGCCGCGGAG TGCGCGCTTGCCGCGCTGTTGCCGGCGCGCGAGGCCACG CAGTTCCTGCGGCCCAGGCAGCGCCGCGCCTTTCAGGTC TTCGAGGAGGCCAAGCAGGGCCACCTGGAGAGGGAGTG CGTGGAGGAGCTGTGCAGCCGCGAGGAGGCGCGGGAGG TGTTCGAGAACGACCCCGAGACGGATTATTTTTACCCAA GATACTTAGACTGCATCAACAAGTATGGGTCTCCGTACA CCAAAAACTCAGGCTTCGCCACCTGCGTGCAAAACCTGC CTGACCAGTGCACGCCCAACCCCTGCGATAGGAAGGGG ACCCAAGCCTGCCAGGACCTCATGGGCAACTTCTTCTGC CTGTGTAAAGCTGGCTGGGGGGGCCGGCTCTGCGACAA AGATGTCAACGAATGCAGCCAGGAGAACGGGGGCTGCC TCCAGATCTGCCACAACAAGCCGGGTAGCTTCCACTGTT

	CCTGCCACAGCGGCTTCGAGCTCTCCTCTGATGGCAGGA CCTGCCAAGACATAGACGAGTGCGCAGACTCGGAGGCC TGCGGGGAGGCGCGCTGCAAGAACCTGCCCGGCTCCTA CTCCTGCCTCTGTGACGAGGGCTTTGCGTACAGCTCCCA GGAGAAGGCTTGCCGAGATGTGGACGAGTGTCTGCAGG GCCGCTGTGAGCAGGTCTGCGTGAACTCCCCAGGGAGC TACACCTGCCACTGTGACGGGCGTGGGGGCCTCAAGCT GTCCCAGGACATGGACACCTGTGAGGACATCTTGCCGTG CGTGCCCTTCAGCGTGGCCAAGAGTGTGAAGTCCTTGTA CCTGGGCCGGATGTTCAGTGGGACCCCCGTGATCCGACT GCGCTTCAAGAGGCTGCAGCCCACCAGGCTGGTAGCTG AGTTTGACTTCCGGACCTTTGACCCCGAGGGCATCCTCC TCTTTGCCGGAGGCCACCAGGACAGCACCTGGATCGTGC TGGCCCTGAGAGCCGGCCGGCTGGAGCTGCAGCTGCGC TACAACGGTGTCGGCCGTGTCACCAGCAGCGGCCCGGT CATCAACCATGGCATGTGGCAGACAATCTCTGTTGAGGA GCTGGCGCGGAATCTGGTCATCAAGGTCAACAGGGATG CTGTCATGAAAATCGCGGTGGCCGGGGACTTGTTCCAAC CGGAGCGAGGACTGTATCATCTGAACCTGACCGTGGGA GGTATTCCCTTCCATGAGAAGGACCTCGTGCAGCCTATA AACCCTCGTCTGGATGGCTGCATGAGGAGCTGGAACTG GCTGAACGGAGAAGACACCACCATCCAGGAAACGGTGA AAGTGAACACGAGGATGCAGTGCTTCTCGGTGACGGAG AGAGGCTCTTTCTACCCCGGGAGCGGCTTCGCCTTCTAC AGCCTGGACTACATGCGGACCCCTCTGGACGTCGGGACT GAATCAACCTGGGAAGTAGAAGTCGTGGCTCACATCCG CCCAGCCGCAGACACAGGCGTGCTGTTTGCGCTCTGGGC CCCCGACCTCCGTGCCGTGCCTCTCTCTGTGGCACTGGT AGACTATCACTCCACGAAGAAACTCAAGAAGCAGCTGG TGGTCCTGGCCGTGGAGCATACGGCCTTGGCCCTAATGG AGATCAAGGTCTGCGACGGCCAAGAGCACGTGGTCACC GTCTCGCTGAGGGACGGTGAGGCCACCCTGGAGGTGGA CGGCACCAGGGGCCAGAGCGAGGTGAGCGCCGCGCAGC TGCAGGAGAGGCTGGCCGTGCTCGAGAGGCACCTGCGG AGCCCCGTGCTCACCTTTGCTGGCGGCCTGCCAGATGTG CCGGTGACTTCAGCGCCAGTCACCGCGTTCTACCGCGGC TGCATGACACTGGAGGTCAACCGGAGGCTGCTGGACCT GGACGAGGCGGCGTACAAGCACAGCGACATCACGGCCC ACTCCTGCCCCCCCGTGGAGCCCGCCGCAGCC
Signal peptide	ATGAATTTACAACCAATTTTCTGGATTGGACTGATCAGT TCAGTTTGCTGTGTGTTTGCTT
Transmembrane peptide	TTATGGGTCATCCTGCTGAGTGCTTTTGCCGGATTGTTGC TGTTAATGCTGCTCATTTTAGCACTGTGG
Linker	GGTGGTGGAGGATCAGGTGGTGGTGGTTCTGGTGGAGG

	TGGAAGT

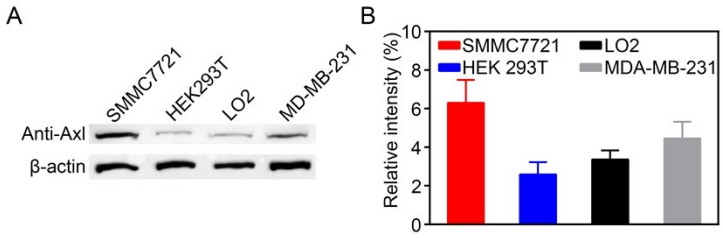

Fig. S1 Axl expression quantity detection of HCC. (A) SMMC7721, MDA-MB-231 (Axl-positive cells), HEK293T, and LO2 (Axl-normal cells) were (A) hybridized with anti-Axl antibody by WB and (B) quantificationally analyzed by using image J.

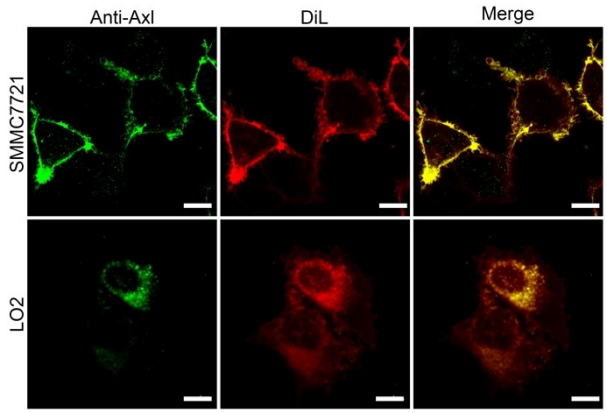

Fig. S2 Immunofluorescence results show that overexpression of Axl on SMMC7721 cell membrane. Scale bar, 10 μm.

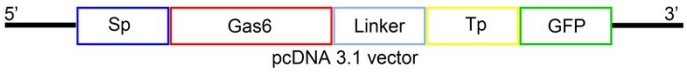

Fig. S3 Schematic illustration of the signal peptide (Sp)-Gas6-transmembrane peptide (Tp)-GFP construct, which is expressed onto the cell membrane.

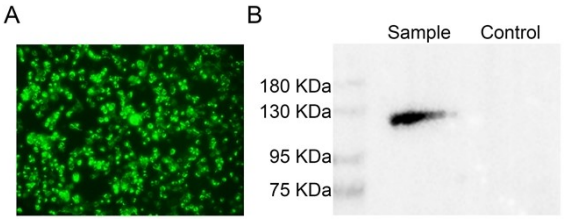

Fig. S4 (A). Transfection efficiency of pcDNA 3.1 vector in HEK293T cells. (B) Western blotting analysis of Gas6 expression on HEK293T cell membrane after plasmids transfection (sample) and HEK293T cell membrane (control).

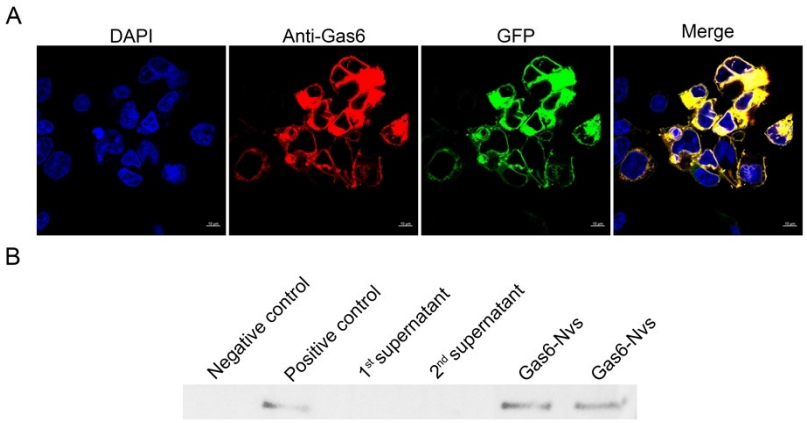

Fig. S5 (A). Immunofluorescence results show that Gas6 expression on HEK293T cell surface. Scale bar, 10 μm. (B) Co-IP and WB analysis of G-Nvs biological activity.

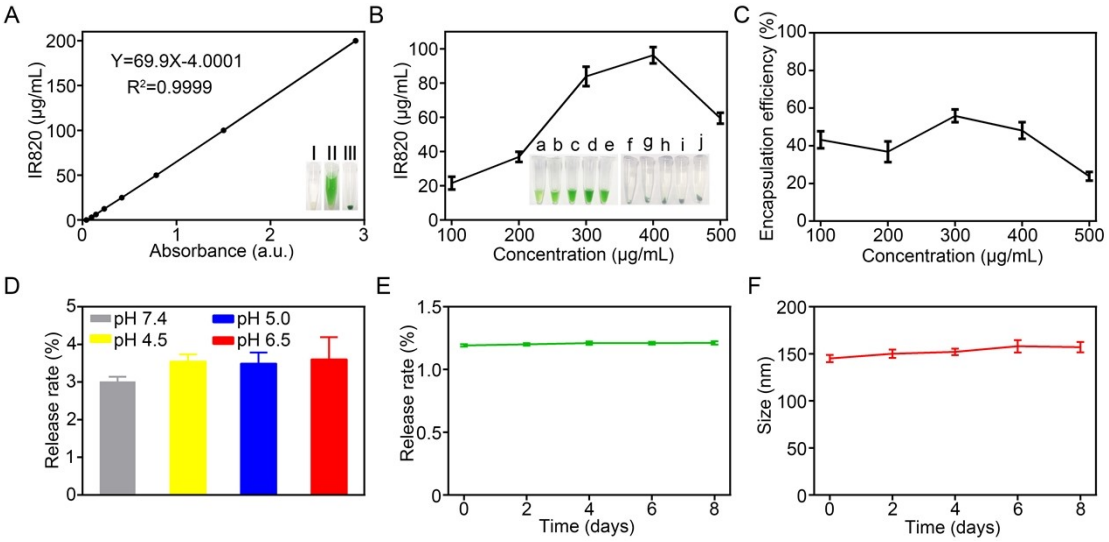

Fig. S6 (A) Standard curve profile of different concentration of free IR820 in deionized water. (I) Insert figure shows transfected cells, (II) transfected cells mixed with free IR820, (III) the synthesis of G-Nvs@IR820. (B) The final concentration of IR820 in the G-Nvs@IR820 were indicated by different IR820 feeding ratio (a/f: 100 μg, b/g: 200 μg, c/h: 300 μg, d/i: 400 μg, e/j: 500 μg). The two groups of tubes are transfected cells (left) and PBS (right), respectively. (C) The encapsulation efficiency of G-Nvs@IR820 in different feeding concentrations of IR820 while transfected cells were fixed at the amount of 10^7. (D) Release rate of G-Nvs@IR820 after different pH treating in the PBS (contain 5% human serum albumin) for 48 h at 37℃. (E) Release rate of G-Nvs@IR820 were measured at 4℃ every two days. (F) Particle size changes of G-Nvs@IR820 at 4℃ were measured every two days.

Fig. S7 (A) UV-vis-NIR absorption spectra of G-Nvs@IR820 dispersed in PBS with various concentrations. (B) Zeta potential analysis of G-Nvs@IR820 and IR820 showing successful IR820 encapsulating in G-Nvs.

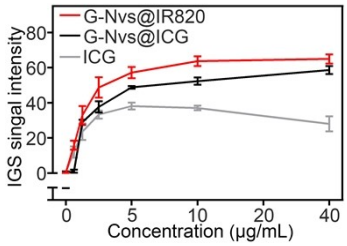

Fig. S8 Fluorescence statistics of NIR dyes of the identical quality. Compared with G-Nvs@IR820, the identical quality of ICG (G-Nvs@ICG, free ICG) showed weaker brightness under surgical navigator.

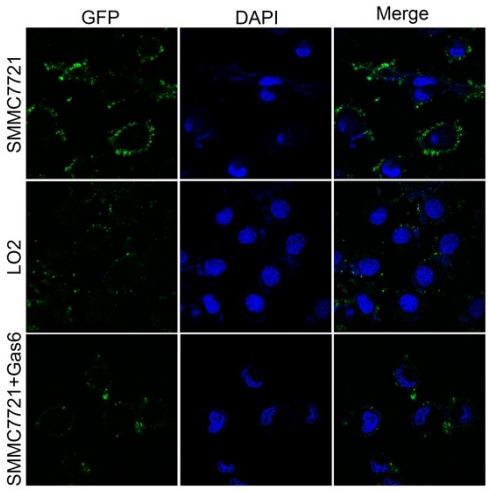

Fig. S9 Cellular binding assay and competitive blocking assay of G-Nvs in SMMC7721 cells (Axl-overexpressing) and LO2 cells (Axl-normal).